

Nonconventional Full-Color Luminescent Polyurethanes: Luminescence Mechanism at the Molecular Orbital Level

Nan Jiang, Ya-Jie Meng, Xin Pu, Chang-Yi Zhu, Shu-Han Tan, Yan-Hong Xu,* You-Liang Zhu,* Jia-Wei Xu, and Martin R. Bryce*



Cite This: *ACS Materials Lett.* 2025, 7, 24–31



Read Online

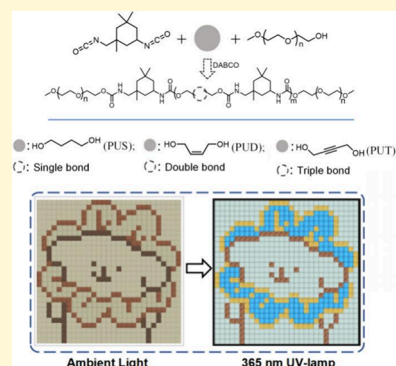
ACCESS |

Metrics & More

Article Recommendations

Supporting Information

ABSTRACT: The study of structure–activity relationships is a top priority in the development of nontraditional luminescent materials. In this work, nonconjugated polyurethanes (PUs) with full-color emission (red, green, and blue) are easily obtained by control of the diol monomer structure and the polymerization conditions. Selected diol monomers introduced single, double, or triple bond repeating units into the main chain of the PUs, in order to understand how unsaturated bonds and H-bonds affect their luminescence from a molecular orbital viewpoint. Detailed experimental and theoretical results show that the PUs have different temperature-dependent behaviors related to the interplay of H-bonding, through-space $n-\pi$ interactions, and aggregation properties. The potential applications of PUs in colorful displays, covert information transmission, and multifunctional bioimaging have been verified. This work provides a new general protocol for the simple preparation of multifunctional nonconventional fluorescent polymers and deepens the understanding of their luminescence mechanisms.



In 1899, the genius inventor Tesla said, “Everything is the light.”¹ People have never stopped pursuing the origins of light and exploiting luminescent phenomena. Traditional luminescent polymers contain large π -conjugated (hetero)-aromatic structures, and through-bond conjugation is the primary source of their emission,^{2,3} in some cases aided by intra- and interchain heteroatom effects.⁴ However, these materials are often complex and expensive to synthesize, require environmentally toxic reagents and catalysts, have limited processability, and are mostly nonbiodegradable, which may significantly restrict their long-term and large-scale applications.^{5–7} However, some nonconjugated luminescent polymers (NCLPs) such as starch, cellulose, and polyacrylate can also emit visible light through noncovalent electronic overlap and delocalization in heteroatom-rich segments.^{5–14} NCLPs with properties such as good biocompatibility, low cost, and good processability are promising materials.^{15–17} A drawback is that they typically emit light of shorter wavelengths (400–500 nm, rarely above 600 nm) and relatively monochromatic light, which greatly limits their application development.^{18–20} Besides, how weak molecular interactions affect the luminescence of NCLPs at the molecular orbital level has always been obscure. Therefore, the simple construction of full-color luminescent NCLPs and in-depth insights into the luminescence mechanism are very timely.

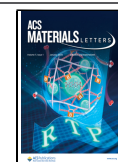
To achieve multicolor luminescence, many studies have relied on the excitation-dependent fluorescence (EDF) of NCLPs, which refers to different emission wavelengths obtained by changing the excitation wavelength.^{21–24} However, this method has several limitations: first, although short-wavelength-excited NCLPs may emit at longer wavelengths, the intensity of the longer-wavelength emissions decreases as the excitation wavelength increases, eventually even approaching zero. Second, many NCLPs do not exhibit EDF characteristics. Third, although EDF may be apparent in the spectral analysis, many commercially available UV lamps emit mixed-wavelength light, unlike lasers or fluorescence spectrometers which typically emit light of a single wavelength. Therefore, in practical applications, changing the excitation wavelength of UV lamps may not result in significant fluorescence changes. Strategies like adjusting through-space interactions between and/or within chains, introducing

Received: October 14, 2024

Revised: November 15, 2024

Accepted: November 15, 2024

Published: November 21, 2024



multiple unconventional chromophores, or changing the relative rigidity and flexibility of the polymer chains have also been used to obtain multicolor NCLPs.^{25–27} Alternatively, the luminescence of NCLPs can be adjusted through heating (including water and air heating).^{28–30} Additionally, due to the abundance of noncovalent interactions, NCLPs are highly susceptible to the influence of the microenvironment, and parameters such as pH can alter their luminescent behavior.^{31–33} However, these external regulatory factors complicate the study of luminescence in NCLPs' aggregated states.

Recently, a new approach to full-color nonconventional luminescence in poly(maleimide) derivatives, without any aromatics, was based on the bonding modes (C–C and C–N linkages) in the backbone.²⁶ We now report a different strategy: namely, intramolecular/intermolecular interactions of polyurethane (PU) chains regulated by introducing single bond (alkane), double bond (alkene), or triple bond (alkyne) repeating units in the backbone lead to full-color emission. Polyurethane is well-known as one of the world's major plastics.³⁴ Different combinations of diisocyanate and diol monomers give PUs with very varied properties and extensive applications in textiles, plastics, electronics, and medical materials.^{35–38} Recent encouraging biodegradability studies make PUs excellent candidates for NCLP developments.^{39,40} In this context, the urethane [–NHCOO–] repeat units provide abundant inter/intrachain interactions conducive to aggregation behavior, electronic overlap and delocalization, such as C=O...N–H (dipole–dipole), C=O...C=O ($n\text{-}\pi^*$), O=C...C=O ($\pi\text{-}\pi^*$), O...O, and hydrogen bonding.^{40–42} Furthermore, the unique soft and hard segment microphase separation structure of PUs gives conformational variability in the aggregated states.^{43,44} Therefore, PUs are ideal templates for tuning multicolor luminescence and studying the aggregation luminescence mechanism.

Nine PU derivatives have now been synthesized by a one-pot reaction of isophorone diisocyanate, poly(ethylene glycol) monomethyl ether, and diol monomers with different central C–C, C=C, or C≡C units (namely, 1,4-butanediol, (Z)-2-butene-1,4-diol, and 2-butyne-1,4-diol). The synthetic route is shown in Figure 1, and structural characterization is detailed in Figures S1–S4. Nuclear magnetic resonance (NMR) spectroscopy shows that all the PUS, PUD, and PUT series are well-structured materials (Figures S1–S3). The molecular weight and molecular weight distribution of the PUs determined by gel permeation chromatography (GPC) show that the products have M_n values in the ranges 2874–2119 (PUS), 3870–2190 (PUD), and 3668–1282 (PUT) (Figure 1 and Table S1). FT-IR spectroscopy (Figure S4) confirmed the presence of a characteristic functional urethane unit. Differential scanning calorimetry (DSC) showed that the introduction of double bonds increased the rigidity of the chain segment and the glass transition temperature (T_g) of the PUD series generally increased compared with the PUS series. However, it is possible that because the introduction of the alkyne group reduces the forces such as bending or entanglement of the soft segments, the PUT series exhibits lower T_g values. Also, maybe due to the low M_n values, the T_g of PUT-b and PUT-c is not obvious (Figure S5).⁴⁵ Thermogravimetric analysis (TGA) established that the PUs have good thermal stability, with a decomposition temperature (T_d 5%) above 221 °C (Figure S6). By simply regulating the reaction temperature in the one-pot reactions, PUs based on different diol linkers, named PUS-a/b/c, PUD-a/b/c, and

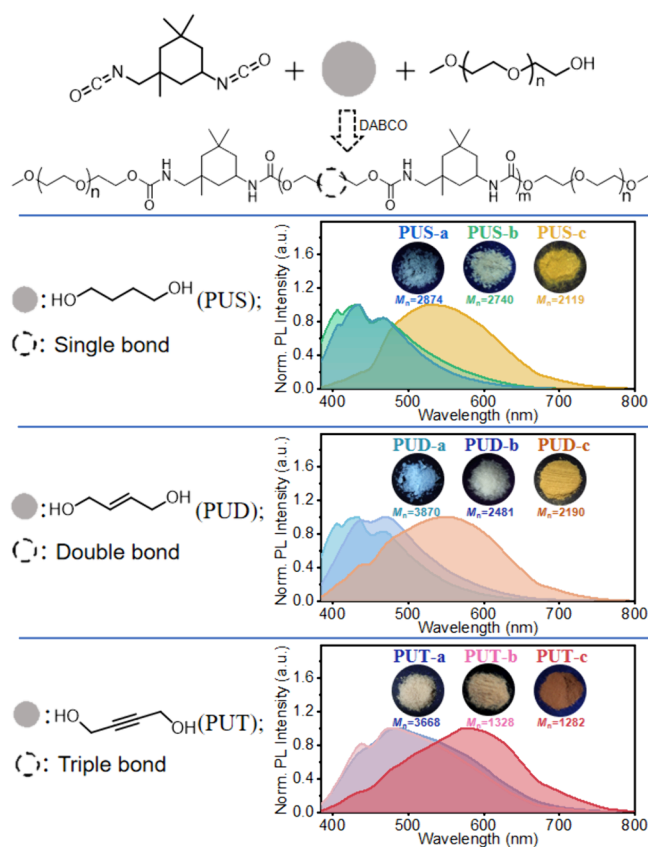


Figure 1. Synthetic route to PUS, PUD, and PUT (S, D, and T = single, double, and triple bond, respectively), the corresponding photoluminescence (PL) spectrum of powdered samples, number-average molecular weight (M_n), and photographs under 365 nm UV illumination.

PUT-a/b/c, respectively, gave different colored emission under a 365 nm UV lamp (Figures 1 and S7).

Within each series (PUS-a/b/c, PUD-a/b/c, and PUT-a/b/c) the polymers all have the same chemical structure; therefore, why are their luminescence properties different? First, the UV–visible absorption and excitation spectra before and after polymerization reactions (Figure S8) showed that the extent of polymerization influenced the width of the spectral profile. In Figure S9, the microscopic morphology of the PUs was monitored by scanning electron microscopy (SEM). Before polymerization, 1,4-butanediol, (Z)-2-butene-1,4-diol, and 2-butyne-1,4-diol monomers showed block/strip thin irregular morphologies. However, after polymerization, PUS-a, PUD-a, and PUT-a showed different degrees of micro-aggregation. PUS-b/c, PUD-b/c, and PUT-b/c showed similar micromorphological changes (Figure S10). Table S3 showed high-temperature products PU-c have higher molar absorbance coefficients than lower-temperature products PU-a/b,⁴⁶ indicating their stronger intermolecular interactions and tighter packing.⁴⁷ The extent of aggregation of the PUs positively correlated with their absorption and emission spectra. The longer wavelength emission of the lower M_n PUs is mainly due to the polymerization reaction whereby the rigid small molecular units become flexible polymer chains, segments of which are entangled, promoting the electron cloud overlap of electron-rich heteroatoms, resulting in strong through-space interactions.^{9,22,48} The fluorescence spectra of the PUs in the solid state showed that with the gradual increase

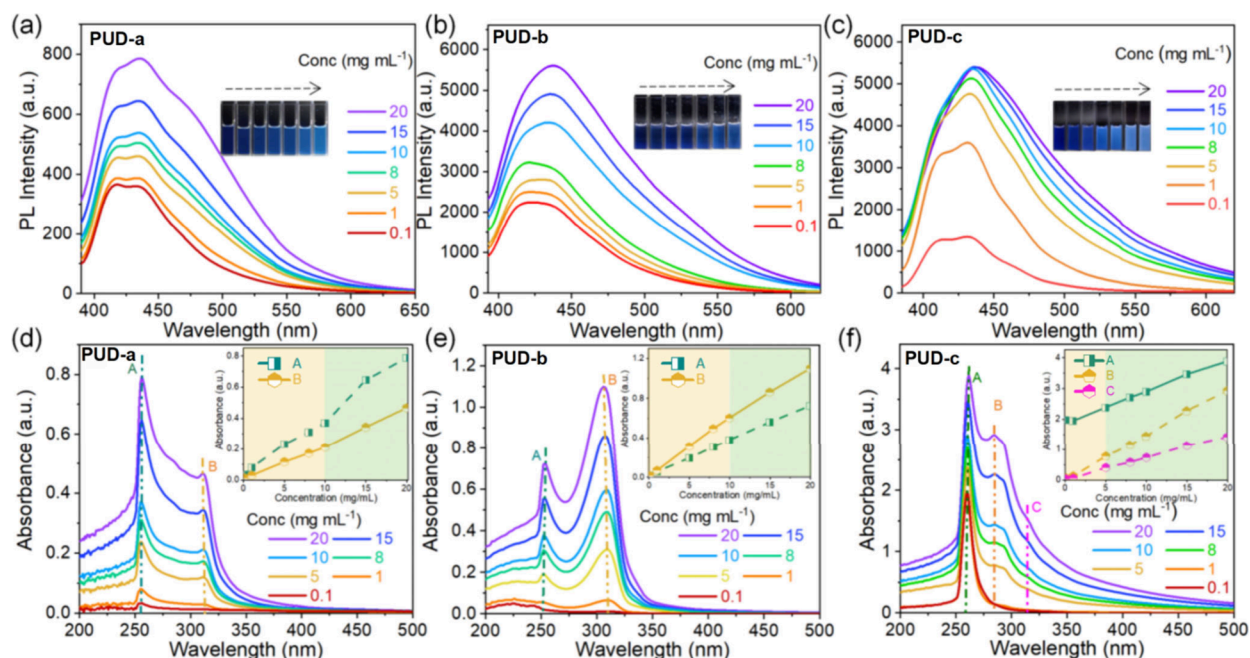


Figure 2. PL spectra of (a) PUD-a, (b) PUD-b, and (c) PUD-c; UV-vis spectra of (d) PUD-a, (e) PUD-b, and (f) PUD-c in DMSO solvent.

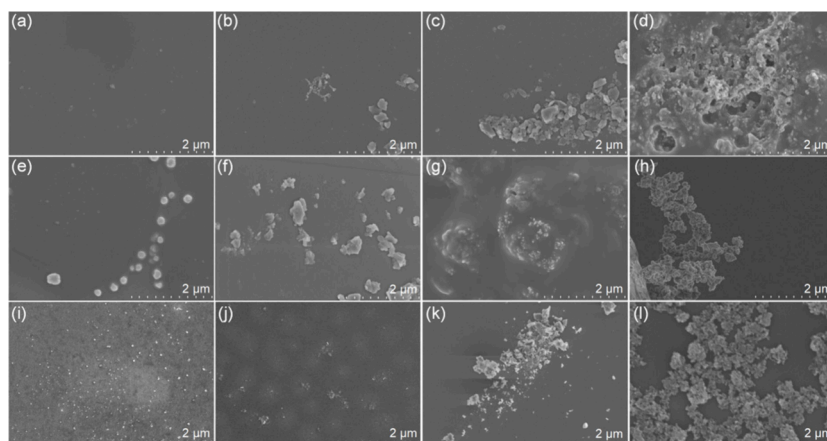


Figure 3. SEM images of PUS-b (a) 0.5 mg mL⁻¹, (b) 1 mg mL⁻¹, (c) 5 mg mL⁻¹, and (d) 10 mg mL⁻¹ in a DMSO solution. SEM images of PUD-b (e) 0.5 mg mL⁻¹, (f) 1 mg mL⁻¹, (g) 5 mg mL⁻¹, and (h) 10 mg mL⁻¹ in DMSO solution. SEM images of PUT-b (i) 0.5 mg mL⁻¹, (j) 1 mg mL⁻¹, (k) 5 mg mL⁻¹, and (l) 10 mg mL⁻¹ in DMSO solution.

of the excitation wavelength, the emission has a significant redshift and excitation-dependent characteristics (Figures S11–S13). The lifetime of the PUS/D/T-c products at different emission peaks and at different excitation wavelengths shows that the emission at different excitation wavelengths comes from different species (Figure S14).^{13,17,19} The absorption and emission behaviors of these samples at different concentrations in DMSO solvent were studied to assess their aggregate luminescence behavior. Figures 2 and S15–S16 show that all the PUs exhibit obvious concentration-enhanced emission characteristics.

The B-peak of the PUs is stable at 300–310 nm (Figures 2 and S15–S16). In PUS and PUT, the position of peak B is stable. However, UV-vis of PUD-c has an extra peak C in place of the original peak B (Figure 2f). Thus, is it possible that peak C is really peak B? Peak B corresponds to S₁, peak A corresponds to S₂, and other minor peaks, such as peak C in Figure 2f and peak C/D in Figure S16e, may be the acromial

peak generated by A/B vibration coupling. The absorption spectra of PUs demonstrate the complex and unpredictable aggregation of the polymer chains. Figure 2d–f shows the aggregation processes of the flexible chain segments at different concentrations and visualizes the existence of multiple emission species after aggregation. The specific content is discussed in the theory section below. Noteworthy, due to the more highly conjugated structure of PUT, the absorption of PUT-c solution exceeding 5 mg mL⁻¹ is beyond the detection range of the instrument (Figure S16f); this also confirms that the spatial electron conjugation within the PUT series is much stronger than for PUS and PUD.

SEM was used to monitor the size and morphological changes of the microscopic aggregates over the concentration change. As shown in Figure 3, PUS, PUD, and PUT showed pronounced concentration-enhanced microscopic aggregation structures. At 0.5 mg mL⁻¹ (Figure 3a,e,i), very sparse and small-sized nanostructures are observed. However, as the

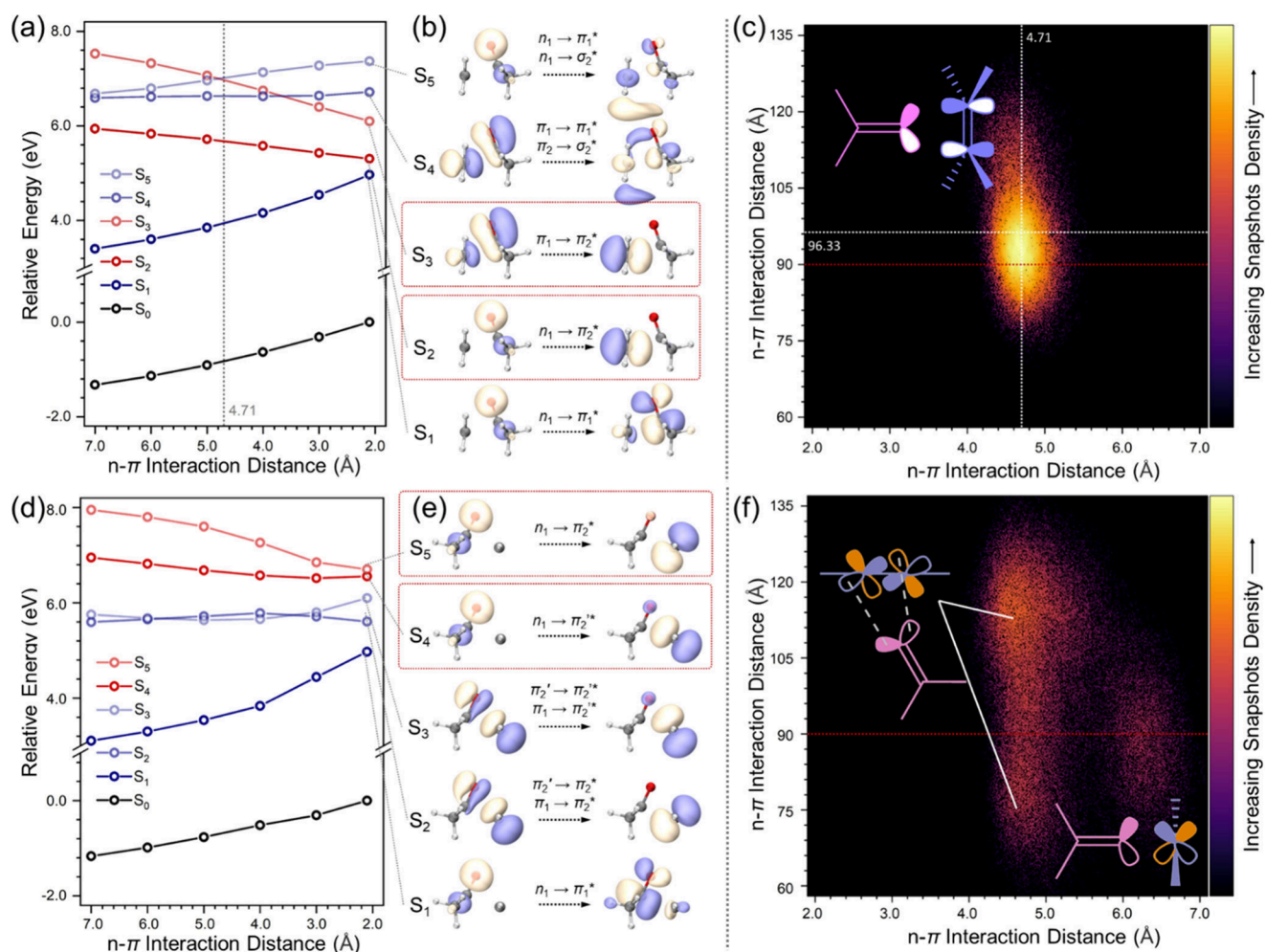


Figure 4. Excited-state level shift in C=O/C=C n- π interaction model system (a) PUD-0, (d) PUT-0. Excitation feature of lowest five excited states for (b) PUD, (e) PUT. Subscripts “1” and “2” denote C=O and C=C moieties, respectively. Density plot of n- π interaction distance and angle in MD3 trajectory of (c) PUD-c, (f) PUT-c.

concentration increased, the PUs continued to aggregate, and at 10 mg mL⁻¹ (Figure 3d,h,l) tightly clustered structures were observed. The accumulation of microscopic aggregates restricts molecular motion and nonradiative pathways, leading to a significant enhancement of fluorescence intensity (Figures 2, S15–S16). In addition, combining the emission characteristics of PUS-c, PUD-c, and PUT-c, it can be inferred that the cluster structure (Figure 3h,l) is more conducive to emission than the sheet structure (Figure 3d), which is reasonable, because the nonconjugated polymer mainly relies on through-space electron communication as the source of luminescence: at this level the cluster is more advantageous than the sheet structure.

Density functional theory (DFT) was used to calculate the lowest unoccupied and highest occupied molecular orbitals (LUMOs and HOMOs) based on two repeating units. As shown in Figure S17, the E_{gap} of PUS, PUD, and PUT decreases successively, consistent with their experimentally observed emission spectra. From the HOMO–LUMO perspective, PUD and PUT are similar; however, their luminous behaviors are quite different. Figure S18 shows that the triple-bonded PUT system has richer and stronger interchain/intrachain interactions, which may result in red-shifted emission. However, the exact source of multicolor emission and the detailed process of how weak interactions

affect nonconjugated chromophores’ luminescence remain unclear (Table S4).

To elucidate the difference in photochemical properties between PUS and PUD/PUT with additional unsaturated moieties, two model systems, namely, PUD-0 (ethylene + acetone) and PUT-0 (acetylene + acetone), were constructed to exclude any influence of the polymer matrix environment. Smooth scan shows that excited state levels are highly related to the n- π interaction distance, i.e., the distance between the midpoints of two π bonds (Figure 4a). The lowest local excitation S_1 state ($n_1 \rightarrow \pi_1^*$, Figure 4b) within C=O changes in parallel with the ground state, indicating that through-space n- π interaction does not influence the $n_1 \rightarrow \pi_1^*$ transition. This corresponds well with the experimental UV–vis spectra, where a stable range of peak B (300–310 nm) is observed in all systems, regardless of the synthetic temperature or the surrounding π^* acceptor (Figures 2, S15–S16). The levels of the S_2 and S_3 states decrease significantly with a smaller interaction distance, showing different behavior compared with other excited states. Natural transition orbitals (NTOs, Figure 4b) show that S_2 and S_3 have a strong through-space charge transfer (TSCT) feature from C=O to C=C, where a lone-pair orbital of an O atom (n_1) or a π orbital of C=O (π_1) acts as a donor in the electronic transition, while a π^* orbital of C=C (π_2^*) acts as an acceptor. Considering that C=O and

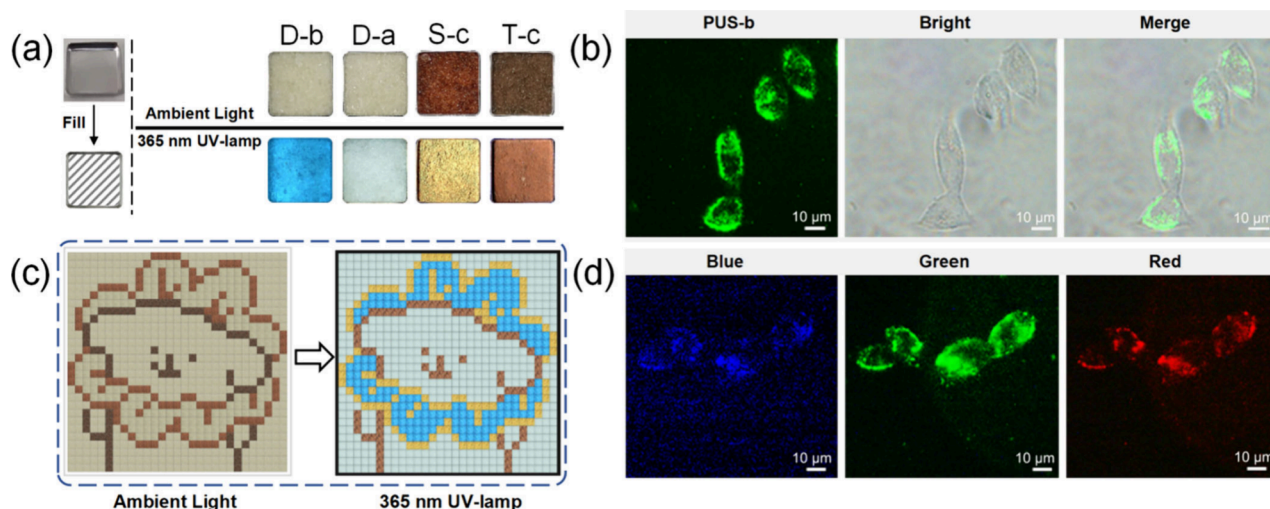


Figure 5. (a) Photographs of PUD-b, PUD-a, PUS-c, and PUT-c in daylight and ultraviolet light. (b) CLSM images of 4T1 cells incubated with $10 \mu\text{g mL}^{-1}$ PUS-b for 6 h under dark field, bright field, and merged images. (c) The pixel painting and its photo in ambient light and 365 nm UV-lamp, respectively. (d) CLSM images of 4T1 cells incubated with $10 \mu\text{g mL}^{-1}$ PUT-c for 6 h under blue, green, and red channels in the cells.

C=C bonds remain perpendicular with each other along the configuration scan, such through-space interactions should be featured as electron donations from n_1 to π_2^* , as shown by the orbital interaction scheme in Figure 4c, with the most efficient overlap when the interaction angle is 90° .

Further MD simulations investigated noncovalent interactions in the aggregated environment. Each system involves a three-stage MD simulation, including (1) MD1: 50.0 ns equilibrium at 298 K, (2) MD2: 1.0 ns heating to synthetic temperature, then followed by 50.0 ns equilibrium, and (3) MD3: 1.0 ns annealing to 298 K, then followed by 50.0 ns equilibrium. As is shown in Figure 4d by density plot, statistics toward MD3 trajectory of PUD-c centers within a specific region, with an average interaction angle of 96.33° , being close to the ideal value of 90° . Since no special treatment was applied for the description of the lone-pair electrons and π^* orbitals in the force field for the simulation, such results demonstrate that the through-space $n-\pi$ interaction is favored by both the intrinsic electric field and the aggregated conformation in PUD. A similar conclusion also holds for PUT (Table S5). The interaction angle for PUT is retained as 96.35° , yet the average through-space $n-\pi$ interaction distance is increased to 6.88 Å, compared with 4.71 Å in PUD. The electron density around $\text{C}\equiv\text{C}$ is higher compared with $\text{C}=\text{C}$; therefore, through-space electron-donation from n_1 to π_2^* is weakened, resulting in a larger interaction distance. In previous work, we have investigated the influence of hydrogen bonding in the aggregated system of nontraditional chromophores.^{49–52} By the formation of a hydrogen bond, the energy level of an n orbital increases to give a lower excitation energy, which should also be considered in PUS/D/T systems. Statistical results suggested that hydrogen bond networks in PU systems generally influence the excitation energy by -1.43 eV.⁵⁰ According to Figure 4b, at the statistical distance (4.71 Å), the excitation energy of the S_2 state in PUD-0 is about 6.4 eV. Taking into account the influence of hydrogen bonds, the excitation energy is expected to be 4.97 eV (250 nm), which corresponds well to the experimental value of the A peak observed in UV-vis spectra (Figure 2) of PUD-a/b/c which originates from $n_1 \rightarrow \pi_2^*$ charge transfer excitation, and both

through-space $n-\pi$ interactions and hydrogen bonds contribute to the color shift. Statistical results of hydrogen bonding and $n-\pi$ interactions during the MD simulations for PUS/D/T show different temperature-dependent behaviors. For hydrogen bonds, a higher synthetic temperature leads to more aggregated structures as discussed,^{49–52} corresponding to an increase in the statistical number from the MD simulations (e.g., 159.8/143.7/173.3 for PUS-a/b/c, respectively). Different from hydrogen bonds, through-space $n-\pi$ interactions show the opposite trend. The same statistical analysis was performed for the C–C bond at the same position of PUS/D/T. For PUS, the statistical number reveals a C–H/C=O interaction at a specific position, which is determined mainly by the electrostatic term and therefore shows a similar trend with hydrogen bonds. However, for PUT, the statistical number involves only through-space $n-\pi$ interaction, showing nonlinear dependence on temperature. In the lower range of synthetic temperatures (PUT-a/b), through-space $n-\pi$ interaction also contributes to more aggregated structures and thus has a similar trend with hydrogen bonds, while as revealed in Figure 4b, a more stable charge transfer excited state is accompanied by an increase in the ground-state energy, making through-space $n-\pi$ interaction disfavored at higher temperature. This is demonstrated by MD simulations at 423 K, where the counts of through-space $n-\pi$ interactions decrease sharply from 585.8 (PUT-b) to 510.1 (PUT-c). These results explain the abnormal photoluminescence (PL) intensity observed in PUT-c. Moreover, for PUD with both C–H/C=O and through-space $n-\pi$ interaction taken into account, opposite temperature-dependent trends result in similar counts of interactions, indicating that PUD should be less sensitive to temperature.

PUT shares similar excited energy trends with PUD, but with the following differences. PUT has more low-lying excited states since $\text{C}\equiv\text{C}$ has two π^* orbitals acting as acceptor. Within the lowest five excited states investigated, there are two targeted $n \rightarrow \pi^*$ transitions (S_4 and S_5 , Figure 4d–f). Although with a similar transition feature, S_4 involves electron transition on two perpendicular orbitals, being slightly lower than S_5 . S_2 and S_3 states show similar mixed features with mainly local

excitation and minor charge transfer. The relative energy levels of S_2 and S_3 share similar energy splitting with the couple of S_4 and S_5 . The n - π interaction in PUT is divided into two major configurations. With shorter n - π interaction distance (4.0–5.0 Å), the interaction angle distributes within a wide range of $70^\circ \sim 130^\circ$, especially two centers can be observed at $\sim 120^\circ$ and $\sim 75^\circ$. Configurations with shorter interaction distance are joined by sloped n - π^* orbital overlap, where two n orbitals of the oxygen atom interact with two carbon atoms (Figure 4f) to ensure efficient overlap. Meanwhile, configurations with longer interaction distance enable n orbitals to interact with π^* at the same carbon atoms, therefore forming a perpendicular interaction angle (centered at $\sim 90^\circ$) and is much weaker than the previous sloped configuration. This can be seen from Figure 4f, where the long-distance configuration shows an obviously lower density. This also explains why PUT-c showed a much lower PL intensity compared with PUT-a/b. With higher temperature, short-distance configuration can be converted into long-distance configuration, while the latter is too weak to maintain a good aggregated structure.

The PUs exhibit different colors under ambient light or under a 365 nm UV lamp. PUD-a, PUD-b, PUS-c, and PUT-c were selected as assembly modules to verify the application potential of PUs in information transmission and colorful displays (Figure 5a). As shown in Figure S18, PUD-a, PUD-b, PUS-c, and PUT-c were used for pixel painting of a dog with a flower scarf. Under ambient light, this painting belongs to the dark series (Figure 5c). However, when illuminated by a 365 nm UV lamp, a bright dog is obtained with a light-blue luminous background, yellowish body, and blue-yellow scarf. PUD-a and PUD-b can also be used to construct a two-dimensional secret information display device (Figures S20–S21). Under daylight, the QR code did not scan any information (Figure S20a). However, under the irradiation of a 365 nm UV lamp, the information is revealed, and the information on “Macromolecules” can be swept out immediately (Figure S20b).

In addition, due to the significant fluorescence and excitation-dependent emission characteristics of the PUs, their potential application in multifunctional bioimaging was explored. Taking PUS-b and PUT-c as examples, as shown in Figure 5b, after being incubated with 4T1 cells for 6 h, PUS-b successfully penetrated the cell membrane, and the cells showed bright green fluorescence, representing an efficient fluorescent probe. 4T1 cells were incubated with $10 \mu\text{g mL}^{-1}$ PUT-c (with both the longest wavelength emission and the strongest excitation-dependent property among the PUs) for 6 h, and then the cells were captured by confocal laser scanning microscopy (CLSM) under three channels. Figure 5d showed bright fluorescence in the 4T1 cells under blue, green, and red channels. MTT assay showed that PUS-b and PUT-c have negligible cytotoxicity toward 4T1 cells (Figure S22), demonstrating their biological safety. Multichannel fluorescence imaging is a valuable tool for better studying biological processes,⁵³ and PUs can, therefore, be considered as a promising multifunctional fluorescence probe.

In summary, this comprehensive study of polyurethane (PU) derivatives with single, double, or triple bond repeating units in the main chain has identified how the different effects of H-bonds and through-space n - π interactions achieve full-color luminescence (red, green, and blue). The detailed photophysical characterization and theoretical calculations reveal that the excited-state levels are highly related to the n -

π interaction distances. The short-wavelength absorption observed in PUD-a/b/c originates from $n_1 \rightarrow \pi_2^*$ charge transfer excitation, and both through-space n - π interactions and hydrogen bonds contribute to the long-wavelength absorption. Such through-space n - π interactions are favored by both the intrinsic electric field and the aggregated conformation in PUD. Statistical results of hydrogen bonding and n - π interactions during the MD simulations for PUS/D/T show different temperature-dependent behaviors. For hydrogen bonds, a higher synthetic temperature leads to better aggregated structures. Through-space n - π interactions show a similar trend in a lower range of synthetic temperature; however, higher temperature disfavored stable through-space n - π interactions, resulting in a decrease in PL intensity and quantum yield. The potential applications of the PUs in colorful displays, covert information transmission, and multifunctional bioimaging have been verified. This work provides a new protocol for the simple preparation of multifunctional fluorescent polymers, while also deepening the understanding of the mechanism of luminescence in the aggregated state of nonconventional luminophores.

■ ASSOCIATED CONTENT

Data Availability Statement

The data associated with this article is available in the manuscript and Supporting Information files.

SI Supporting Information

The Supporting Information is available free of charge at <https://pubs.acs.org/doi/10.1021/acsmaterialslett.4c02100>.

Experimental section; structure analysis; additional photophysical data; scanning electron microscopy (SEM) data; computational data (PDF)

■ AUTHOR INFORMATION

Corresponding Authors

Yan-Hong Xu – Key Laboratory of Preparation and Applications of Environmental Friendly Materials, Key Laboratory of Functional Materials Physics and Chemistry of the Ministry of Education, Jilin Normal University, Changchun 130103, China; orcid.org/0000-0002-9930-587X; Email: xuyh198@163.com

You-Liang Zhu – State Key Laboratory of Supramolecular Structure and Materials, College of Chemistry, Jilin University, Changchun 130012, China; orcid.org/0000-0002-9561-0770; Email: youliangzhu@jlu.edu.cn

Martin R. Bryce – Department of Chemistry, Durham University, Durham DH1 3LE, U.K.; orcid.org/0000-0003-2097-7823; Email: m.r.bryce@durham.ac.uk

Authors

Nan Jiang – Key Laboratory of Preparation and Applications of Environmental Friendly Materials, Key Laboratory of Functional Materials Physics and Chemistry of the Ministry of Education, Jilin Normal University, Changchun 130103, China

Ya-Jie Meng – Ministry-of-Education Key Laboratory of Numerical Simulation of Large-Scale Complex System (NSLSCS) and School of Chemistry and Materials Science, Nanjing Normal University, Nanjing 210023, China

Xin Pu – State Key Laboratory of Supramolecular Structure and Materials, College of Chemistry, Jilin University, Changchun 130012, China

Chang-Yi Zhu – Key Laboratory of Preparation and Applications of Environmental Friendly Materials, Key Laboratory of Functional Materials Physics and Chemistry of the Ministry of Education, Jilin Normal University, Changchun 130103, China

Shu-Han Tan – Key Laboratory of Preparation and Applications of Environmental Friendly Materials, Key Laboratory of Functional Materials Physics and Chemistry of the Ministry of Education, Jilin Normal University, Changchun 130103, China

Jia-Wei Xu – Ministry-of-Education Key Laboratory of Numerical Simulation of Large-Scale Complex System (NSLSCS) and School of Chemistry and Materials Science, Nanjing Normal University, Nanjing 210023, China;
orcid.org/0000-0002-2732-086X

Complete contact information is available at:

<https://pubs.acs.org/10.1021/acsmaterialslett.4c02100>

Author Contributions

Nan Jiang and Ya-Jie Meng contributed equally to this work. All authors have given approval to the final version of the manuscript. CRediT: Nan Jiang conceptualization, data curation, investigation, writing-original draft; Chang-Yi Zhu and Shu-Han Tan formal analysis, methodology; Ya-Jie Meng, Jia-Wei Xu, Xin Pu, and You-Liang Zhu conceptualization, software; Yan-Hong Xu writing-review and editing; Martin R. Bryce conceptualization, supervision, writing-review and editing.

Notes

The authors declare no competing financial interest.

ACKNOWLEDGMENTS

The work was funded by the Science and Technology Development Program of Jilin Province (YDZJ202301-ZYTS305). M.R.B. thanks EPSRC grant EP/L02621X/1 for funding.

REFERENCES

- (1) Csanyi, E. Interview with Nikola Tesla (1899). In *Electrical Engineering Portal*. <https://electrical-engineering-portal.com/nikola-tesla-everything-is-the-light>. (accessed 2024-11-14).
- (2) Grimsdale, A. C.; Leok Chan, K.; Martin, R. E.; Jokisz, P. G.; Holmes, A. B. Synthesis of Light-Emitting Conjugated Polymers for Applications in Electroluminescent Devices. *Chem. Rev.* **2009**, *109*, 897–1091.
- (3) Mortimer, R. J.; Dyer, A. L.; Reynolds, J. R. Electrochromic Organic and Polymeric Materials for Display Applications. *Displays* **2006**, *27*, 2–18.
- (4) Cameron, J.; Kanibolotsky, A. L.; Skabara, P. J. Lest We Forget-The Importance of Heteroatom Interactions in Heterocyclic Conjugated Systems, from Synthetic Metals to Organic Semiconductors. *Adv. Mater.* **2024**, *36*, 2302259.
- (5) Tomalia, D. A.; Klajnert-Maculewicz, B.; Johnson, K. A.-M.; Brinkman, H. F.; Janaszewska, A.; Hedstrand, D. M. Non-Traditional Intrinsic Luminescence: Inexplicable Blue Fluorescence Observed for Dendrimers, Macromolecules and Small Molecular Structures Lacking Traditional/Conventional Luminophores. *Prog. Polym. Sci.* **2019**, *90*, 35–117.
- (6) Luo, J.; Guo, S.; Chen, F.; Jiang, B.; Wei, L.; Gong, Y.; Zhang, B.; Liu, Y.; Wei, C.; Tang, B. Z. Rational Design Strategies for Nonconventional Luminogens with Efficient and Tunable Emission in Dilute Solution. *Chem. Eng. J.* **2023**, *454*, 140469.
- (7) Jiang, N.; Zhu, D. X.; Su, Z. M.; Bryce, M. R. Recent Advances in Oligomers/Polymers with Unconventional Chromophores. *Mater. Chem. Front.* **2021**, *5*, 60–75.
- (8) Lai, W. F. Non-Aromatic Clusteroluminogenic Polymers: Structural Design and Applications in Bioactive Agent Delivery. *Mater. Today Chem.* **2022**, *23*, 100712–100725.
- (9) Hu, C.; Guo, Z.; Ru, Y.; Song, W.; Liu, Z.; Zhang, X.; Qiao, J. A New Family of Photoluminescent Polymers with Dual Chromophores. *Macromol. Rapid Commun.* **2018**, *39*, 1800035–1800041.
- (10) Wang, R.; Yuan, W.; Zhu, X. Aggregation-Induced Emission of Non-Conjugated Poly(Amido Amine)s: Discovering, Luminescent Mechanism Understanding and Bioapplication. *Chin. J. Polym. Sci.* **2015**, *33*, 680–687.
- (11) Du, L. L.; Jiang, B. L.; Chen, X. H.; Wang, Y. Z.; Zou, L. M.; Liu, Y. L.; Gong, Y. Y.; Wei, C.; Yuan, W. Z. Clustering-Triggered Emission of Cellulose and Its Derivatives. *Chin. J. Polym. Sci.* **2019**, *37*, 409–415.
- (12) Jiang, N.; Zhu, C. Y.; Li, K. X.; Xu, Y. H.; Bryce, M. R. Recent Progress in Nonconventional Luminescent Macromolecules and their Applications. *Macromolecules* **2024**, *57*, 5561–5577.
- (13) Bauri, K.; Saha, B.; Banerjee, A.; De, P. Recent Advances in the Development and Applications of Nonconventional Luminescent Polymers. *Polym. Chem.* **2020**, *11*, 7293–7315.
- (14) Wang, Z.; Zhang, H. K.; Li, S. Q.; Lei, D. Y.; Tang, B. Z.; Ye, R. Q. Recent Advances in Clusteroluminescence. *Topics Curr. Chem.* **2021**, *379*, 14–36.
- (15) Chen, X.; He, Z.; Kausar, F.; Chen, G.; Zhang, Y.; Yuan, W. Z. Aggregation-Induced Dual Emission and Unusual Luminescence beyond Excimer Emission of Poly(Ethylene Terephthalate). *Macromolecules* **2018**, *51*, 9035–9042.
- (16) Pucci, A.; Rausa, R.; Ciardelli, F. Aggregation-Induced Luminescence of Polyisobutene Succinic Anhydrides and Imides. *Macromol. Chem. Phys.* **2008**, *209*, 900–906.
- (17) Tang, S. X.; Yang, T. J.; Zhao, Z. H.; Zhu, T. W.; Zhang, Q.; Hou, W. B. W.; Yuan, W. Z. Nonconventional Luminophores: Characteristics, Advancements and Perspectives. *Chem. Soc. Rev.* **2021**, *50*, 12616–12655.
- (18) Shang, C.; Zhao, Y. X.; Long, J. Y.; Ji, Y.; Wang, H. L. Orange-Red and White-Emitting Nonconventional Luminescent Polymers Containing Cyclic Acid Anhydride and Lactam Groups. *J. Mater. Chem. C* **2020**, *8*, 1017–1024.
- (19) Sakhno, T. V.; Sakhno, Yu. E.; Kuchmiy, S. Ya. Clusteroluminescence of Unconjugated Polymers: A Review. *Theor. Exp. Chem.* **2023**, *59*, 75–106.
- (20) Deng, J.; Jia, H.; Xie, W.; Wu, H.; Li, J.; Wang, H. Nontraditional Organic/Polymeric Luminogens with Red-Shifted Fluorescence Emissions. *Macromol. Chem. Phys.* **2022**, *223*, 2100425–2100439.
- (21) Shang, C.; Wei, N.; Zhuo, H. M.; Shao, Y. M.; Zhang, Q.; Zhang, Z. X.; Wang, H. L. Highly Emissive Poly(Maleic Anhydride-Alt-Vinyl Pyrrolidone) with Molecular Weight-Dependent and Excitation-Dependent Fluorescence. *J. Mater. Chem. C* **2017**, *5*, 8082–8090.
- (22) Wang, H.; Li, Q.; Alam, P.; Bai, H.; Bhalla, V.; Bryce, M. R.; Cao, M.; Chen, C.; Chen, S.; Chen, X.; Chen, Y.; Chen, Z.; Dang, D.; Ding, D.; Ding, S.; Duo, Y.; Gao, M.; He, W.; He, X.; Hong, X.; Hong, Y.; Hu, J. J.; Hu, R.; Huang, X.; James, T. D.; Jiang, X.; Konishi, G.; Kwok, R. T. K.; Lam, J. W. Y.; Li, C.; Li, H.; Li, K.; Li, N.; Li, W. J.; Li, Y.; Liang, X. J.; Liang, Y.; Liu, B.; Liu, G.; Liu, X.; Lou, X.; Lou, X. Y.; Luo, L.; McGonigal, P. R.; Mao, Z. W.; Niu, G.; Owyong, T. C.; Pucci, A.; Qian, J.; Qin, A.; Qiu, Z.; Rogach, A. L.; Situ, B.; Tanaka, K.; Tang, Y.; Wang, B.; Wang, D.; Wang, J.; Wang, W.; Wang, W. X.; Wang, W. J.; Wang, X.; Wang, Y. F.; Wu, S.; Wu, Y.; Xiong, Y.; Xu, R.; Yan, C.; Yan, S.; Yang, H. B.; Yang, L. L.; Yang, M.; Yang, Y. W.; Yoon, J.; Zang, S. Q.; Zhang, J.; Zhang, P.; Zhang, T.; Zhang, X.; Zhang, X.; Zhao, N.; Zhao, Z.; Zheng, J.; Zheng, L.; Zheng, Z.; Zhu, M. Q.; Zhu, W. H.; Zou, H.; Tang, B. Z. Aggregation-Induced Emission (AIE), Life and Health. *ACS Nano* **2023**, *17*, 14347–14405.

- (23) Chu, B.; Liu, X.; Xiong, Z.; Zhang, Z.; Liu, B.; Sun, J.; Yang, Q.; Zhang, H.; Zhang, C.; Zhang, X.; Tang, B. Z. Near-Infrared Clusteroluminescence in Amine-Capped Polyesters. *ChemRxiv*, 2023. DOI: 10.26434/chemrxiv-2023-fdwc6 (accessed 2024-11-14).
- (24) Liao, P.; Huang, J.; Yan, Y.; Tang, B. Z. Clusterization-Triggered Emission (CTE): One for All, All for One. *Mater. Chem. Front.* **2021**, *5*, 6693–6717.
- (25) Zhang, H.; Tang, B. Z. Through-Space Interactions in Clusteroluminescence. *JACS Au* **2021**, *1*, 1805–1814.
- (26) Ji, X.; Tian, W. G.; Jin, K. F.; Diao, H. L.; Huang, X.; Song, G. J.; Zhang, J. Anionic Polymerization of Nonaromatic Maleimide to Achieve Full-Color Nonconventional Luminescence. *Nat. Commun.* **2022**, *13*, 3717–3729.
- (27) Chu, B.; Zhang, H.; Hu, L.; Liu, B.; Zhang, C.; Zhang, X.; Tang, B. Z. Altering Chain Flexibility of Aliphatic Polyesters for Yellow-Green Clusteroluminescence in 38% Quantum Yield. *Angew. Chem., Int. Ed.* **2022**, *134*, No. e202114117.
- (28) Zhao, Y.; Long, P.; Zhuang, P.; Ji, Y.; He, C.; Wang, H. Transforming Polyethylene and Polypropylene into Nontraditional Fluorescent Polymers by Thermal Oxidation. *J. Mater. Chem. C* **2022**, *10*, 1010–1016.
- (29) Zhao, Y.; Xie, W.; Deng, J.; Liu, D.; Liu, H.; Li, T.; Wang, H. A Gas-Thermal Method as a Universal and Convenient Strategy for Preparing Non-Traditional Luminescent Polymers with Enhanced and Red-Shifted Fluorescence. *New J. Chem.* **2023**, *47*, 15005–15009.
- (30) Chen, X.; Hu, C.; Wang, Y.; Li, T.; Jiang, J.; Huang, J.; Wang, S.; Liu, T.; Dong, W.; Qiao, J. Tunable Red Clusteroluminescence Polymers Prepared by a Simple Heating Process. *ACS Appl. Mater. Interfaces* **2023**, *15*, 23824–23833.
- (31) Liu, P.; Fu, W.; Verwilt, P.; Won, M.; Shin, J.; Cai, Z.; Tong, B.; Shi, J.; Dong, Y.; Kim, J. S. MDM2-Associated Clusterization-Triggered Emission and Apoptosis Induction Effectuated by a Theranostic Spiropolymer. *Angew. Chem., Int. Ed.* **2020**, *59*, 8435–8439.
- (32) Yang, T.; Zhou, J.; Shan, B.; Li, L.; Zhu, C.; Ma, C.; Gao, H.; Chen, G.; Zhang, K.; Wu, P. Hydrated Hydroxide Complex Dominates the AIE Properties of Nonconjugated Polymeric Luminophores. *Macromol. Rapid Commun.* **2022**, *43*, 2100720–2100728.
- (33) Xie, Y.; Liu, D.; Zhang, H.; Wang, D.; Zhao, Z.; Tang, B. Z. Clusteroluminescence in Maleimide: From Well-Known Phenomenon to Unknown Mechanism. *ChemRxiv*, 2022. (accessed 2024-11-14). DOI: 10.26434/chemrxiv-2022-vznv4
- (34) Niesiołędzka, J.; Datta, J. Challenges and Recent Advances in Bio-Based Isocyanate Production. *Green Chem.* **2023**, *25*, 2482–2504.
- (35) Ju, D. B.; Lee, J. C.; Hwang, S. K.; Cho, C. S.; Kim, H. J. Progress of Polysaccharide-Contained Polyurethanes for Biomedical Applications. *Tissue Eng. Regen. Med.* **2022**, *19*, 891–912.
- (36) Phung Hai, T. A.; Tessman, M.; Neelakantan, N.; Samoylov, A. A.; Ito, Y.; Rajput, B. S.; Pourahmady, N.; Burkart, M. D. Renewable Polyurethanes from Sustainable Biological Precursors. *Biomacromolecules* **2021**, *22*, 1770–1794.
- (37) Wendels, S.; Averous, L. Biobased Polyurethanes for Biomedical Applications. *Bioac. Mater.* **2021**, *6*, 1083–1106.
- (38) Jiang, N.; Li, G. F.; Zhang, B. H.; Zhu, D. X.; Su, Z. M.; Bryce, M. R. Aggregation-Induced Long-Lived Phosphorescence in Non-conjugated Polyurethane Derivatives at 77 K. *Macromolecules* **2018**, *51*, 4178–4184.
- (39) Bhavsar, P.; Bhav, M.; Webb, H. K. Solving the Plastic Dilemma: the Fungal and Bacterial Biodegradability of Polyurethanes. *World J. Microbiol. Biotechnol.* **2023**, *39*, 122.
- (40) Jiang, N.; Li, K. X.; Wang, J. J.; Zhu, Y. L.; Zhu, C. Y.; Xu, Y. H.; Bryce, M. R. Amphiphilic Polyurethane with Cluster-Induced Emission for Multichannel Bioimaging in Living Cell Systems. *ACS Macro Lett.* **2024**, *13*, 52–57.
- (41) Jiang, N.; Ruan, S. H.; Liu, X. M.; Zhu, D. X.; Li, B.; Bryce, M. R. Supramolecular Oligourethane Gel with Multicolor Luminescence Controlled by Mechanically Sensitive Hydrogen-Bonding. *Chem. Mater.* **2020**, *32*, 5776–5784.
- (42) Cui, B.; Wu, Q. Y.; Gu, L.; Shen, L.; Yu, H. B. High Performance Bio-based Polyurethane Elastomers: Effect of Different Soft and Hard Segments. *Chinese. J. Polym. Sci.* **2016**, *34*, 901–909.
- (43) Liu, S.; Yuan, Y.; Li, J. Y.; Sun, S. Q.; Chen, Y. L. An Optomechanical Study of Mechanoluminescent Elastomeric Polyurethanes with Different Hard Segments. *Polym. Chem.* **2020**, *11*, 1877–1884.
- (44) Aoki, D.; Yoshida, H.; Ajiro, H. Comb Polyurethanes Consisting of Hard Segment Backbones and Dangling Soft Segments for Tailoring Mechanical Properties of Thermoplastics. *Macromolecules* **2024**, *57*, 640–651.
- (45) Pei, H. Y.; Liu, Y. L.; Wang, D. F.; Wang, J.; Wang, C. J.; Wu, Y. Z.; Pan, W.; Su, C. H.; Song, M.; Cao, S. K. All-Optical Non-Conjugated Multi-Functionalized Photorefractive Polymers via Ring-Opening Metathesis Polymerization. *e-Polym.* **2020**, *20*, 353–360.
- (46) Siu, H.; Duhamel, J. Molar Absorbance Coefficient of Pyrene Aggregates in Water Generated by a Poly(Ethylene Oxide) Capped at a Single End with Pyrene. *J. Phys. Chem. B* **2012**, *116*, 1226–1233.
- (47) Gu, X.; Zeng, R.; Hou, Y.; Yu, N.; Qiao, J.; Li, H.; Wei, Y.; He, T.; Zhu, J.; Deng, J.; Tan, S.; Zhang, C.; Cai, Y.; Long, G.; Hao, X.; Tang, Z.; Liu, F.; Zhang, X.; Huang, H. Precisely Regulating Intermolecular Interactions and Molecular Packing of Nonfused-Ring Electron Acceptors via Halogen Transposition for High-Performance Organic Solar Cells. *Angew. Chem., Int. Ed.* **2024**, *63*, No. e202407355.
- (48) Li, Q. Q.; Tang, Y. H.; Hu, W. P.; Li, Z. Fluorescence of Nonaromatic Organic Systems and Room Temperature Phosphorescence of Organic Luminogens: The Intrinsic Principle and Recent Progress. *Small* **2018**, *14*, 1801560–1801579.
- (49) Jiang, N.; Meng, Y. J.; Zhu, C. Y.; Li, K. X.; Li, X.; Xu, Y. H.; Xu, J. W.; Bryce, M. R. Nonconjugated Polyurethane Derivatives with Aggregation-Induced Luminochromism for Multicolor and White Photoluminescent Films. *ACS Macro Lett.* **2024**, *13*, 1226–1232.
- (50) Jiang, N.; Pu, X.; Li, K. X.; Zhu, C. Y.; Sun, Y. W.; Xu, Y. H.; Zhu, Y. L.; Bryce, M. R. One-Pot Preparation of Nonconventional Luminescent Polymer Gels Driven by Polymerization. *Polym. Chem.* **2024**, *15*, 4101.
- (51) Li, K. X.; Meng, Y. J.; Zhu, C. Y.; Jiang, N.; Xu, J. W.; Xu, Y. H. Tunable Multicolor Fluorescence of Polyurethane Derivatives Controlled by Molecular Weight. *Polym. Chem.* **2024**, *15*, 2235–2239.
- (52) Jiang, N.; Li, K. X.; Wang, J. J.; Li, C. S.; Xu, X. Y.; Xu, Y. H.; Bryce, M. R. Cluster-Induced Aggregation in Polyurethane Derivatives with Multicolour Emission and Ultra-Long Organic Room Temperature Phosphorescence. *J. Mater. Chem. C* **2024**, *12*, 1040–1046.
- (53) Rodriguez-Sevilla, P.; Thompson, S. A.; Jaque, D. Multichannel Fluorescence Microscopy: Advantages of Going Beyond a Single Emission. *Adv. NanoBiomed. Res.* **2022**, *2*, 2100084.